

# NUMERICAL SIMULATIONS OF REGIONAL WAVE PROPAGATION IN REALISTIC EARTH MODELS

Gregory S. Wagner & Thomas J. Owens  
Department of Geological Sciences  
University of South Carolina  
Columbia, SC 29208

AFOSR Contract No. F49620 - 94 - 1 - 0066

## Abstract

Preliminary results for numerical simulations of regional propagation in realistic earth models are presented. The modeling is motivated in part by three-component array observations which show that the  $P$  and  $S$  codas, and  $L_g$  wavetrains for regional sources are comprised of substantial amounts of forward scattered/multipathed energy, and in part by results from numerical simulations of teleseismic wave propagation which suggest a correlation between the coda level and rate of decay and the aspect ratio of lithospheric heterogeneities. Numerical simulations are conducted using a two-dimensional, fourth order accurate,  $P$ - $SV$  finite difference routine. The models consist of a heterogeneous layer over a homogeneous half-space. Perturbations are in velocity and parameterized using a gaussian correlation function.

The wavefields generated using models containing high aspect ratio heterogeneities (ANISO) exhibit several characteristic consistent with regional array observations. First, the  $Pg$  wavetrain and coda consists of forward scattered, coherent plane wave energy trapped in the crustal waveguide. Models containing isotropic heterogeneities (ISO) inhibit the extent to which energy is trapped in the crustal waveguide and produce codas dominated by randomly scattered energy. Waveforms generated using models containing ANISO heterogeneities exhibit another feature commonly observed in regional array data. That is, that detailed features in waveforms observed at adjacent sensors exhibit a high degree of coherence, while those observed at sensors separated by distances on the order of a wavelength exhibit a somewhat surprising loss of coherence. Waveforms generated using models containing ISO heterogeneities exhibit a degree of incoherence inconsistent with regional array observations.

The modeling results presented in this report add to the growing body of evidence illustrating the important role spatially anisotropic heterogeneities play in seismic wave propagation and scattering. An important but overlooked implication inherent in parameterizing heterogeneities with spatially anisotropic correlation functions is that the dimensionless normalized wavenumber  $ka$  commonly used to categorize the scattering regime loses its meaning. Estimates of the effective scattering cross section and the associated scattering radiation pattern need include the vector quantity  $\mathbf{k} \cdot \mathbf{a}$  to reflect the fact that the nature of scattering depends not only on the (scalar) ratio of the "size" of the heterogeneities to the wavelength of the incident wavefield, but also on the spatial relation/orientation of the incident wavefield and heterogeneities.

**key words:** *regional wave propagation, scattering, seismic coda, spatially anisotropic heterogeneities, heterogeneity aspect ratio.*

- **Objective**

The main objective of our research is to provide an improved understanding of regional wave propagation and to aid in the characterization of lithospheric heterogeneities by combining analysis of observed three-component array data and numerical simulations of elastic wave propagation in realistic earth structures.

- **Preliminary Research Results**

This report provides preliminary results from numerical simulations of regional wave propagation in realistic earth structures. The modeling is motivated in part by three-component array observations which show that the  $P$  and  $S$  codas, and  $L_g$  wavetrains for regional sources are comprised of a considerable amount of forward scattered/multipathed energy (Wagner & Owens, 1993, 1995a,b; Dainty & Schultz, 1995), and in part by results from numerical simulations of teleseismic wave propagation which suggest a correlation between the coda level and rate of decay and the aspect ratio of lithospheric heterogeneities (Wagner & Langston, 1992). The results presented in this report are simply an extension of the teleseismic modeling to the regional problem in an effort to determine the types of structure required to produce wavefields that exhibit the same characteristics observed in regional array data.

The basic model used in our investigation is a heterogeneous layer (*i.e.* lithosphere) over a homogeneous half-space (*i.e.* mantle). The use of this general model for both teleseismic and regional simulations is motivated by the assumption that small scale heterogeneities are generally confined to the lithosphere. The heterogeneities are parameterized using a gaussian correlation function (space domain  $\leftrightarrow$  wavenumber domain)

$$\exp \left[ -(x^2 + z^2)/(a_x^2 + a_z^2) \right] \quad \longleftrightarrow \quad \frac{(a_x^2 + a_z^2)}{2} \exp \left[ -(k_x^2 a_x^2 + k_z^2 a_z^2)/4 \right] \quad (1)$$

where  $a_x$ ,  $a_z$  are the horizontal and vertical correlation distances, respectively. The two end members of this model parameterization scheme are models with isotropic heterogeneities (ISO) and models with homogeneous plane layers. As the aspect ratio ( $a_x/a_z$ ) increases, the heterogeneities are stretched in the horizontal direction. Heterogeneities with higher aspect ratios (ANISO) mimic plane layers of varying lateral extent. These types of models are intuitively appealing because they agree with geologic models where layers do not have infinite lateral extent but are truncated by faulting, pinch outs, *etc.* Figure 1 shows examples of ISO and ANISO models; the correlation distances are  $a_x=a_z=5$  km for the ISO model, and  $a_x=50$  km,  $a_z=5$  km for the ANISO model.

The results presented in this report are for models whose heterogeneities consist of correlated  $P$  and  $S$  velocity perturbations. The mean  $P$  and  $S$  velocities are, respectively, 5.25 and 3.03 km/s in the layer, and 7.50 and 4.33 km/s in the half-space. The standard deviation of the  $P$  and  $S$  velocity perturbations is 5% of their respective background means. The density is 2.5 kg/m<sup>3</sup> for both the layer and the half-space. No intrinsic attenuation is included in the model.

Numerical methods are currently the only methods available to compute waveforms in a medium whose properties vary both laterally and vertically in a random manner. Simulations were performed using a two-dimensional, fourth-order accurate, displacement,  $P$ - $SV$  finite difference (FD) routine. Because our main objective was to identify models that will produce predominantly forward as opposed to back scattered codas, it was crucial that we use a numerical approach capable of modeling both the forward and back-scattered components of the wavefield. Absorbing boundary conditions (Clayton & Engquist, 1977) are used on the sides and bottom of the model, and

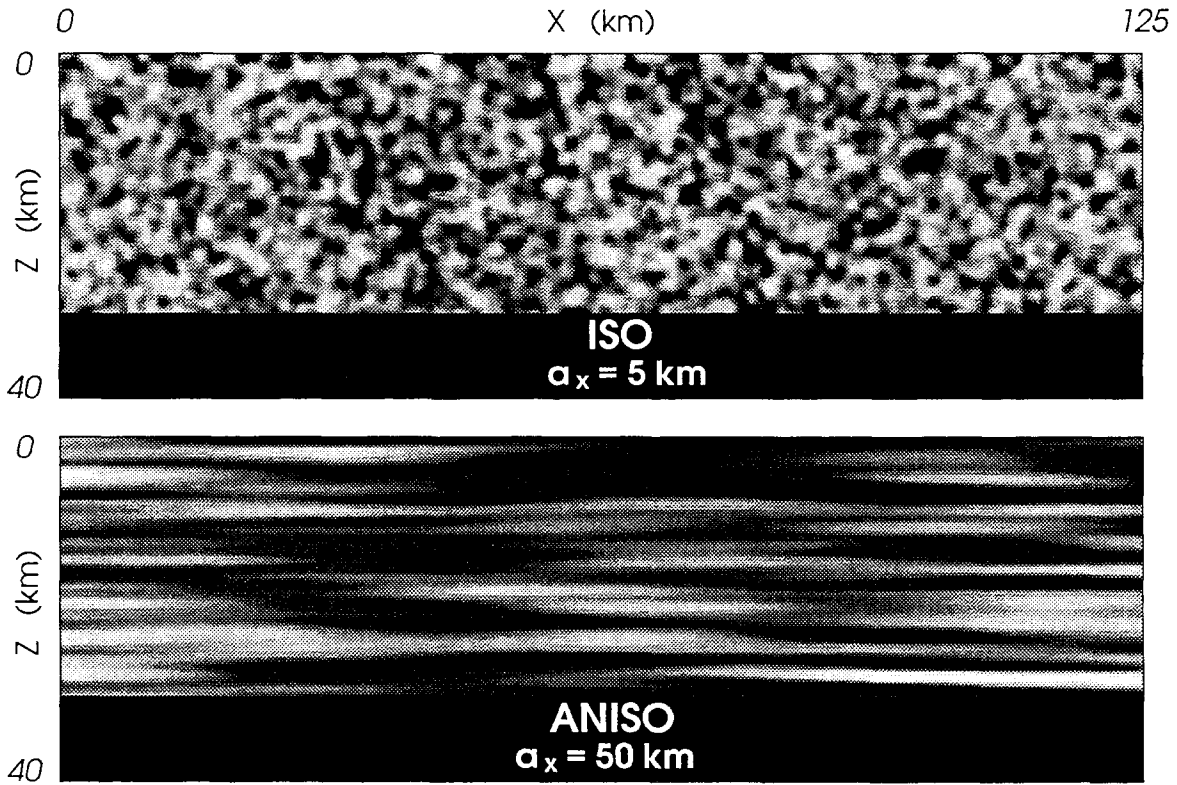


Figure 1: Examples of models with spatially isotropic (ISO) and spatially anisotropic (ANISO) heterogeneities. The perturbations are parameterized using a gaussian correlation function. The ISO model (top) has spatially isotropic heterogeneities with a correlation distance of 5 km. The ANISO model (bottom) has spatially anisotropic heterogeneities with vertical and horizontal correlation distances of 5 km and 50 km, respectively.

stress-free boundary conditions (Ilan & Loewenthal, 1976) at the surface. The source is an isotropic gaussian at a depth of 5 km.

Figures 2 and 3 show the vertical and horizontal component snap-shots for the ANISO and ISO models, respectively (note that each frame is normalized to its respective maximum; time in seconds is listed to the right). While Figures 2 and 3 do not show propagation to regional distances (only to 125 km here), it is clear that the salient wavefield features are established at this early stage. Figures 2 and 3 illustrate two important differences in the wavefields associated with these two models. First, the wavefield generated using the ANISO model is consistent with regional array observations in that it consists largely of forward scattered, coherent plane wave energy (note also the coherent plane wave nature of the energy entering the "mantle"). The wavefield generated using the ISO model is, conversely, dominated by randomly scattered energy. The few plane waves generated in the ISO model are the direct, and the  $P$  and  $P$ -to- $SV$  converted waves reflected/refracted at the layer/half-space interface and the free surface. While we certainly would not suggest that the ISO model represents a reasonable model for lithospheric structure, it is clear that models with ISO heterogeneities inhibit the development of wavefields with characteristics consistent with observed array data. The heterogeneity aspect ratio appears to play the key role in determining the extent to which energy is forward scattered and, consequently, trapped in the crustal waveguide.

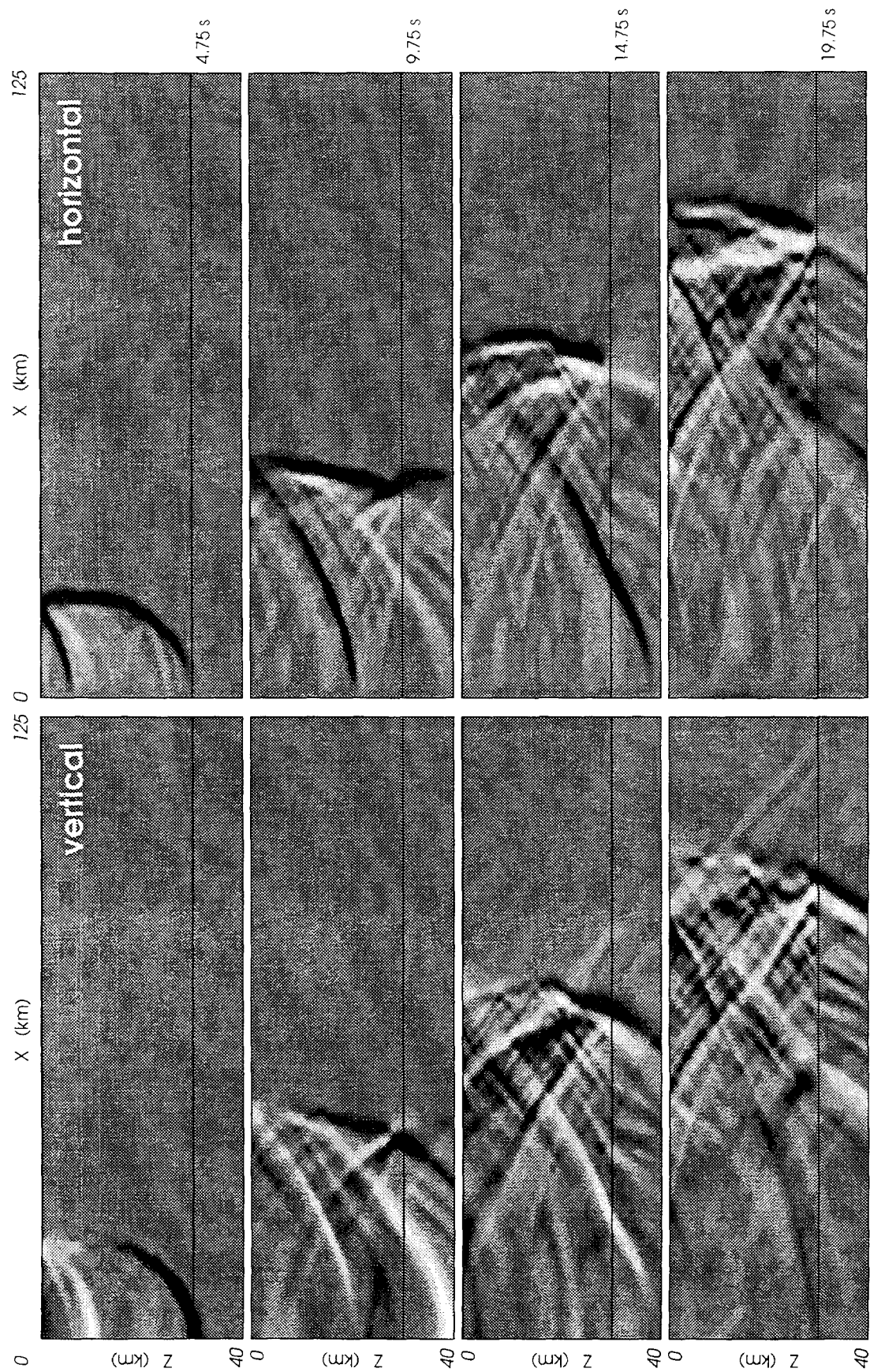


Figure 2: Vertical (left) and horizontal (right) component snap-shots for propagation through the model with spatially anisotropic heterogeneities (see Figure 1). Each frame is normalized to its respective maximum. Time, in seconds, is listed to the right. Note that the P-coda is dominated by coherent, forward scattered plane waves, a characteristic feature observed in both local and regional array data.



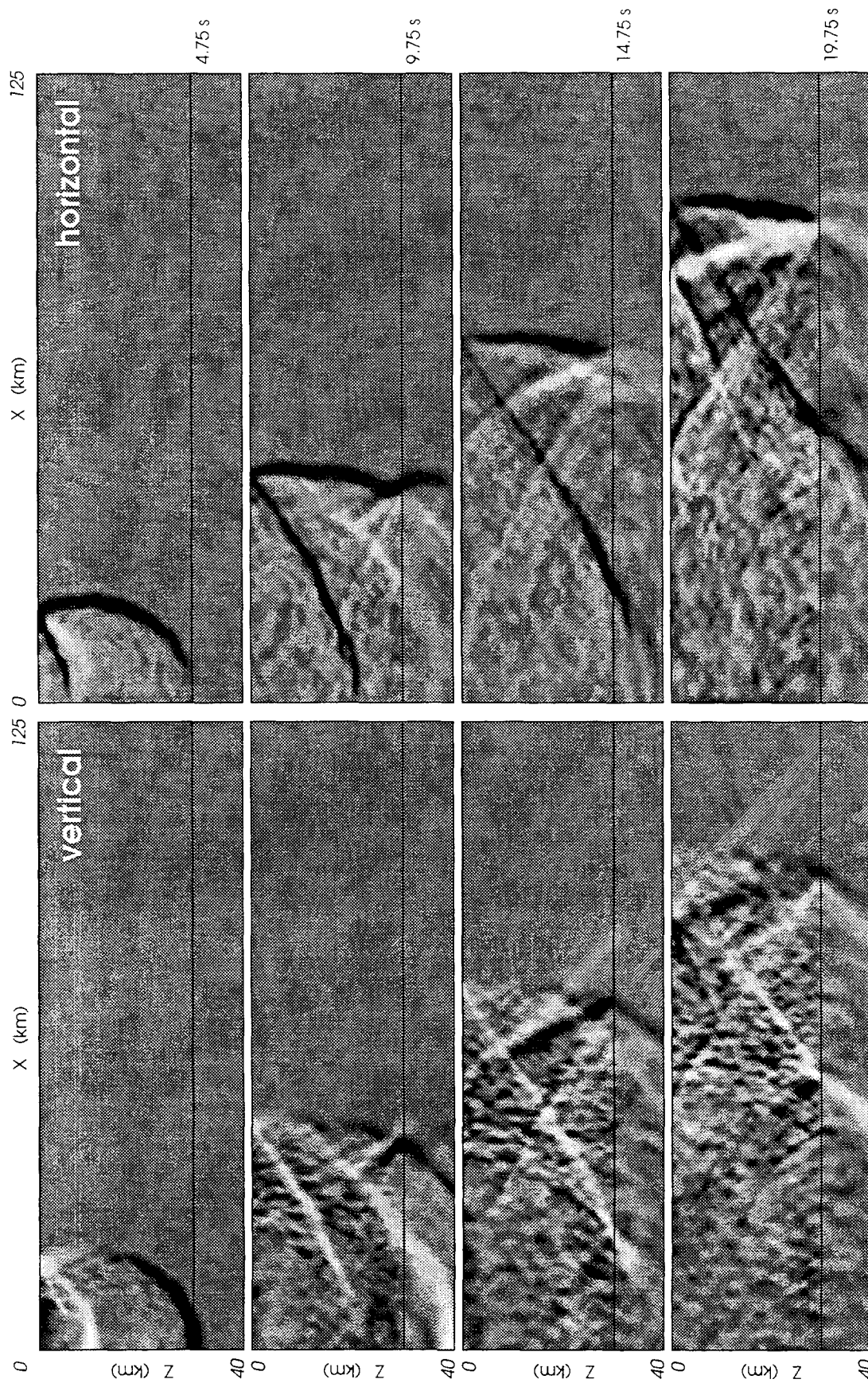


Figure 3: Vertical (left) and horizontal (right) component snap-shots for propagation through the model with spatially isotropic heterogeneities (see Figure 1). Each frame is normalized to its respective maximum. Time, in seconds, is listed to the right. Note that the P-coda is dominated by randomly scattered energy, this feature is inconsistent with array observations for both local and regional sources.

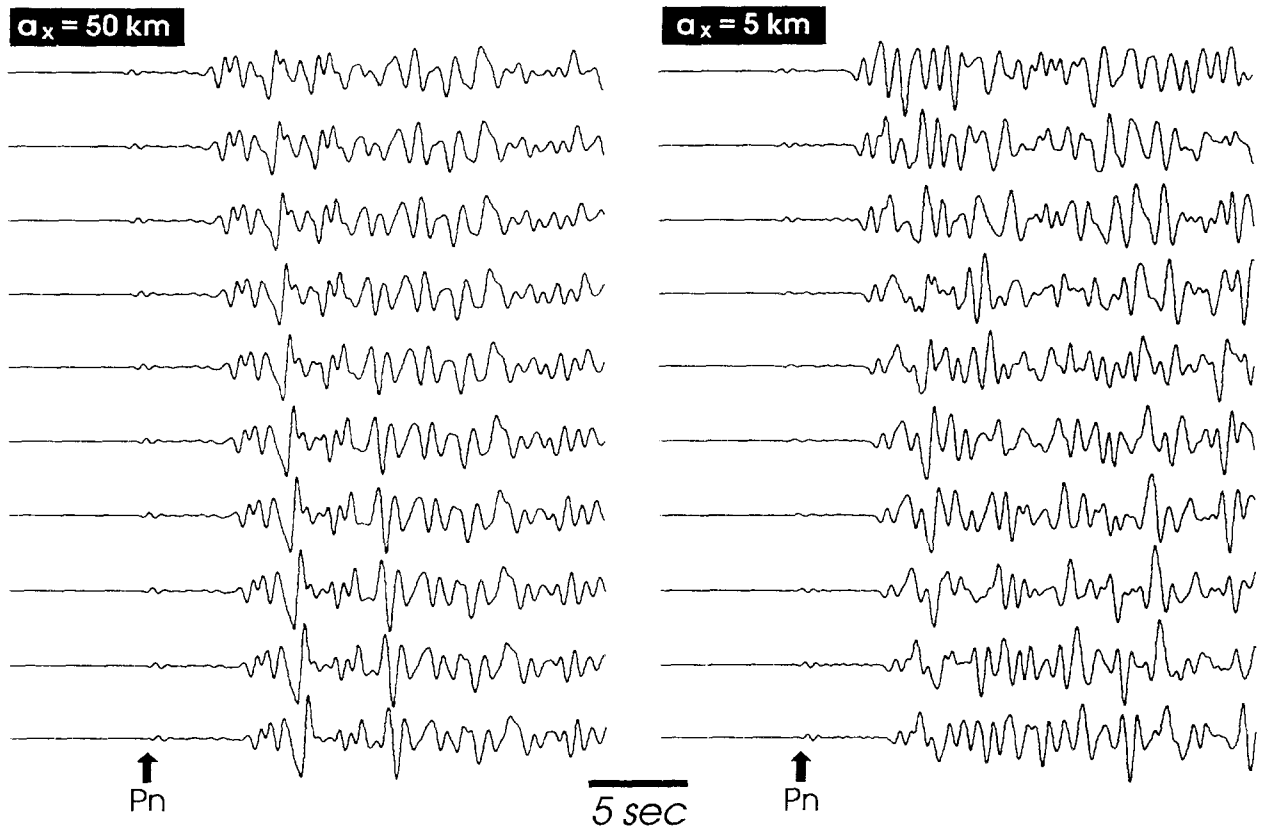


Figure 4: Vertical component (velocity)  $P_n$ ,  $P_g$  and  $P_g$ -coda waveforms generated using the ANISO (left) and ISO models (right) shown in Figure 1. Sensor spacing is 1 km. Source distance increases from top (250 km) to bottom (260 km).

The second significant difference illustrated in Figures 2 and 3 is that the ANISO model facilitates the excitation of considerable source zone reverberations. This feature coupled with other structural effects, such as scattering from topographic features, could conceivably result in enhanced contributions to the regional wavefield from source zone scattering (Greenfield, 1971).

Figure 4 shows the vertical component (velocity) waveforms generated using the ANISO (left) and ISO models (right) observed at 250–260 km. Because we used a  $P$  source we limit attention to the  $P_n$  and  $P_g$  wavetrains and codas. The  $P_n$  for both models are similar and rather nondescript.  $P_n$  coda is not readily produced in either of the models, both of which have homogeneous "mantles". The implication here is that  $P_n$  coda is not the product of  $P_n$  scattering in the crust, but  $P_n$  scattering that occurs in the upper mantle. Presumably, therefore, the addition of ANISO heterogeneities to the upper-mantle would be needed to generate forward scattered  $P_n$  coda.

The  $P_g$  wavetrain and coda generated using the ANISO model exhibit several characteristics observed in regional array data. First is simply the extended coherent nature of  $P_g$ . There is no one distinct  $P_g$  arrival but several equal amplitude arrivals, some of which may be a direct result of the aforementioned source zone reverberations, that have traveled slightly different crustal paths from source to receiver (Kennett, 1989). The second similarity between the ANISO and observed array data is that subtle feature in waveforms observed at adjacent sensors exhibit a high degree of coherence, while those observed at sensors separated by distances on the order of a wavelength exhibit an unexpected reduction in correlation, and those observed at sensors separated by several

wavelengths are seemingly unrelated. The waveforms generated using the ISO model exhibit a degree of sensor-wise incoherence inconsistent with regional array observations. In fact, the  $P_g$  wavetrain generated using the ISO model exhibits almost no coherent coda. Both the extended nature and slow spatial evolution of the ANISO model's  $P_g$  wavetrain result from the interaction and interference of the numerous forward scattered plane waves generated by scattering from the spatially anisotropic heterogeneities and trapped in the crustal waveguide and, potentially, the numerous smaller waveguides bound by the spatially anisotropic heterogeneities.

## • Conclusions & Future Plans

The FD modeling outlined in this report was conducted in an effort to determine the type of structures capable of producing regional wavefields with characteristics consistent with those observed in regional three-component array data. Namely, wavefields whose  $P$  and  $S$  codas, and  $L_g$  wavetrains contain significant amounts of forward scattered/multipathed energy. The use of models with spatially anisotropic heterogeneities was motivated by previous results from simulations of teleseismic wave propagation. For the teleseismic case, the heterogeneity aspect ratio appears to play an important role in determining the coda level and rate of decay by controlling the extent to which vertically propagating energy is scattered into the horizontal direction. The modeling results presented in this report suggest that for the regional case, the heterogeneity aspect ratio plays an important role in determining the extent to which energy is forward scattered and, consequently, trapped in the crustal waveguide. It is this feature, the presence of waves such as  $P_g$  and  $L_g$  comprised of energy trapped in the crustal waveguide, that differentiates the regional wavefield from local and teleseismic wavefields. Models with spatially anisotropic heterogeneities not only produce wavefields consistent with array observations, but also provide a physically and intuitively appealing way to parameterize earth structure.

The modeling results presented in this report add to the growing body of evidence illustrating the important role spatially anisotropic heterogeneities play in seismic wave propagation and scattering (*cf.* Wagner & Langston, 1992; Hestholm *et al.*, 1994; Hoshiya, 1995). An important but overlooked implication inherent in parameterizing heterogeneities with spatially anisotropic correlation functions is that the dimensionless normalized wavenumber  $ka$  commonly used to categorize the scattering regime (*i.e.* Rayleigh, Mie, Fresnel) loses its meaning. Clearly, spatially anisotropic heterogeneities can not be treated as point scatterers. The effective scattering cross section and associated scattering radiation pattern for ANISO heterogeneities depend not only on the physical properties of the heterogeneity (Wu & Aki, 1985), but also need include the vector quantity  $\mathbf{k} \cdot \mathbf{a}$  to reflect the fact that the scattering depends not simply on the scalar ratio of the "size" of the heterogeneities to the wavelength of the incident wavefield, but also on the spatial relation/orientation of the incident wavefield and heterogeneities.

In future modeling, ANISO heterogeneities with varying aspect ratios, standard deviations, physical properties, *etc.*, will be incorporated into models with various background structures such as low velocity surface layers, and surface and layer/half-space boundary topography. Our modeling has also highlighted the limitations of using a two-dimensional routine to investigate what is truly a three-dimensional phenomena. Future modeling will be three-dimensional and include heterogeneities with  $a_x \approx a_y > a_z$ .

## References

- Clayton, R. and Engquist, B., 1977. Absorbing boundary conditions for acoustic and elastic wave equations, *Bull. Seis. Soc. Am.*, **67**(6), 1529–1540.
- Ilan, A. and Loewenthal, D., 1976. Instability of finite difference schemes due to boundary conditions in elastic media, *Geophys. Prosp.*, **24**, 431–453.
- Dainty, A. M. and Schultz, C. A., 1995. Crustal reflections and the nature of regional *P* coda, *Bull. Seis. Soc. Am.*, **85**(3), 851–858.
- Greenfield, R. J., 1971. Short-period P-wave generation by Rayleigh-wave scattering at Novaya Zemlya, *J. Geophys. Res.*, **76**(32), 7988–8001.
- Hestholm, S. O., Husebye, E. S., and Ruud, B. O., 1994. Seismic wave propagation in complex crust-upper mantle media using 2-D finite-difference synthetics, *Geophys. J. Int.*, **118**, 643–670.
- Hoshiba, M., 1995. Estimation of nonisotropic scattering in western Japan using coda wave envelopes: application of a multiple nonisotropic scattering model, *J. Geophys. Res.*, **100**(B1), 645–657.
- Kennett, B. L. N., 1989. On the nature of regional seismic phases—I. phase representations for  $P_n, P_g, S_n, L_g$ , *Geophys. J. R. astr. Soc.*, **98**, 447–456.
- Wagner, G. S. and Langston, C. A., 1992. A numerical investigation of scattering effects for teleseismic plane wave propagation in a heterogeneous layer over a homogeneous half-space, *Geophys. J. Int.*, **110**, 486–500.
- Wagner, G. S. and Owens, T. J., 1993. Broadband bearing-time records of three-component seismic array data and their application to the study of local earthquake coda, *Geophys. Res. Letters*, **20**(17), 1823–1826.
- Wagner, G. S. and Owens, T. J., 1995a. Broadband eigen-analysis for three-component seismic array data, *IEEE Trans. on Signal Processing*, **43**(7), 1738–1741.
- Wagner, G. S. and Owens, T. J., 1995b. Regional wavefield analysis using three-component seismic array data, *Proceedings 17th Annual Seismic Research Symposium*. PL-TR-95-2108
- Wu, R-S. and Aki, K., 1985. Scattering characteristics of elastic waves by an elastic heterogeneity, *Geophysics*, **50**(4), 582–595.